

# Semiparametric Growth-Curve Modeling in Hierarchical, Longitudinal Studies

Rajesh Selukar

SAS Institute Inc., Cary NC  
rajesh.selukar@sas.com

## Abstract

Modeling of growth (or decay) curves arises in many fields such as microbiology, epidemiology, marketing, and econometrics. Parametric forms like Logistic and Gompertz are often used for modeling such monotonic patterns. While useful for compact description, the real-life growth curves rarely follow these parametric forms perfectly. Therefore, the curve estimation methods that strike a balance between prior information in the parametric form and fidelity with the observed data are preferred. In hierarchical, longitudinal studies the interest lies in comparing the growth curves of different groups while accounting for the differences between the within-group subjects. This article describes a flexible state space modeling framework that enables semiparametric growth curve modeling for the data generated from hierarchical, longitudinal studies. The methodology, a type of functional mixed effects modeling, is illustrated with a real-life example of bacterial growth in different settings.

*Keywords*— Growth Curve, Semiparametric Modeling, State Space Model, Longitudinal Data

## 1 Introduction

Study of growth and decay patterns arises in many fields. For example, microbiologists study the growth of bacteria in different settings, epidemiologists study the increase in the number of infected patients after a disease outbreak and, chemists study the decay of the active agents in chemical compounds to determine their shelf lives. The analysis of experimental or observational data from such studies is used for a variety of purposes, such as, validating the understanding of the inner workings of the process, comparing the growth/decay patterns in different settings, extrapolating the growth patterns in the future, and so on.

An important step in such analysis is the estimation of the underlying growth (decay) curves. Parametric forms like Logistic and Gompertz, as well as nonparametric forms such as smoothing splines, are often used for modeling such monotonic patterns. The usefulness and popularity of parametric approach is clear from the large

number of R packages available in the Comprehensive R Archive Network (CRAN), which support parametric growth-curve modeling. A good summary of the state of art in the parametric growth-curve modeling is provided in Garre et al. [2023], which describes the functionality of an R package, *biogrowth*. In nonparametric growth curve modeling, smoothing splines with and without monotonicity constraints is a popular approach, e.g., see, Ramsay [1988], Chan et al. [2021] and the references therein. In Harvey and Kattuman [2020], the spread of COVID-19 cases is modeled using a state space modeling based approach. They, however, model the growth rate (derivative of the growth curve) rather than the growth curve itself. All these references, with the exception of Garre et al. [2023], are primarily concerned with the modeling of a single growth curve. In hierarchical, longitudinal studies, multiple growth curves are generated as a result of monitoring multiple subjects from a group (or multiple groups). In such cases the interest lies in estimating the group-mean-curves, after accounting for the subject specific differences. For these types of problems the dominant approaches have been based on linear mixed-effects, nonlinear mixed-effects, and functional mixed-effects modeling, e.g., see Fine et al. [2019], Blozis and Harring [2016]. In these references, when linear mixed-effects or functional mixed-effects models are used, the group-mean-curves are often linear or polynomial smoothing splines, which, while flexible, do not use the prior monotonicity information of the growth curves. In nonlinear mixed-effects modeling, it is assumed that the subject curves are generated by parametric growth curve models such as Logistic and some or all of the model parameters, like the growth rate, for each subject are assumed to be random perturbations of their mean population values. However, in this case, the subject curves being fully parametric can be a restrictive assumption.

In this article, the analysis of multiple growth curves generated by hierarchical, longitudinal studies is done using functional mixed-effects (FME) modeling. An FME model for growth curves decomposes a subject specific curve as follows:

$$\text{subject-curve} = \text{group-mean-curve} + \text{regression-effects} + \\ \text{deviation-from-mean-curve} + \text{noise}$$

The group-mean-curve, which is expected to follow a growth curve pattern, is called a functional fixed-effect, the deviation-from-mean-curve is called a functional random-effect, regression-effects can either be fixed or random, and the noise is a zero-mean, Gaussian error term. In this article, the group-mean-curve is modeled semiparametrically according to a simple modification of the state space model based approach described in section 3 of Ansley et al. [1993]. Our modification makes their approach computationally feasible in much wider settings. Making their elegant growth curve modeling approach easily accessible to the wider applied research community is one of the goals of this article. All the FME models considered in this article are formulated as linear, Gaussian, state space models, SSMs for short. This provides many additional advantages such as modeling flexibility, computational efficiency, and easy interpretability (see Guo [2002], Selukar [2015]). The analysis for the illustrations in this article is carried out by using the CSSM procedure in the SAS Viya/Econometrics software, see SAS. The data and the SAS code used for these illustrations is available on request.

The remainder of the article is organized as follows: Section 2 lays out the required SSM framework (the parametric growth curve formulation is in Section 2.1, the semiparametric formulation is in Section 2.2, and the FME model formulation is in Section 2.3), Section 3 contains an example that explains the methodology, and finally Section 4 concludes.

Table 1: Examples of  $g(\boldsymbol{\theta}, t)$  in Popular Growth/Decay Curves

Name	$g(\boldsymbol{\theta}, t)$	Parameter Vector $\boldsymbol{\theta}$
Linear	$t$	
Exponential	$\exp(-\rho t)$	$\rho$
Logistic	$\frac{1}{(1+\phi \exp(-\rho t))}$	$\phi, \rho$
Gompertz	$\exp(-\phi \exp(-\rho t))$	$\phi, \rho$
Richards	$(1 + \phi \exp(-\rho t))^{(-1/\nu)}$	$\phi, \rho, \nu$

## 2 State Space Modeling Framework

SSMs have long been used to model a variety of sequential data, such as time series, panels of time series, and longitudinal data. Many different forms of SSMs are used in practice. In order to handle the formulation of FME models for the longitudinal data, this article uses an SSM form that is similar to the one described in chap. 6, sec. 4 of Durbin and Koopman [2012]. The notation and additional details are included in the appendix, Appendix A.

In this article when vectors and matrices are described in inline mode, they are written row-wise with rows separated by semicolons.

### 2.1 SSM Formulation of a Parametric Growth Curve

Let  $y_t$  denote noisy measurements on a growth/decay curve  $f(\boldsymbol{\theta}, t)$ . That is,

$$y_t = f(\boldsymbol{\theta}, t) + \epsilon_t \tag{1}$$

where  $\epsilon_t$  is a noise sequence of independent, zero-mean, Gaussian variables with variance  $\sigma_\epsilon^2$ , and the latent curve,  $f(\boldsymbol{\theta}, t) = \text{constant} + \text{scale } g(\boldsymbol{\theta}, t)$ , is a smooth, monotonic function of  $t$ , which might depend on some parameter vector  $\boldsymbol{\theta}$ ; *constant* and *scale* are auxiliary parameters that do not depend on  $\boldsymbol{\theta}$ . A few popular choices of  $g(\boldsymbol{\theta}, t)$  are shown in Table 1; several more examples can be found in Zwietering et al. [1990]. When the functional form of the latent curve,  $f(\boldsymbol{\theta}, t)$ , is completely known, the unknown parameters,  $(\text{constant}, \text{scale}, \boldsymbol{\theta}, \sigma_\epsilon^2)$ , can be estimated by nonlinear least-squares. Alternatively, the estimation of  $f(\boldsymbol{\theta}, t)$  can be accomplished by using the SSM form of Equation 1, which has many additional advantages. The SSM form is based on a simple two-dimensional recursion. Suppressing  $\boldsymbol{\theta}$  for notational simplicity,  $f(t+h) = \text{constant} + \text{scale } g(t+h)$  can be expressed in terms of  $f(t)$  as

$$\begin{bmatrix} \text{constant} + \text{scale } g(t+h) \\ \text{scale} \end{bmatrix} = \begin{bmatrix} 1 & (g(t+h) - g(t)) \\ 0 & 1 \end{bmatrix} \begin{bmatrix} \text{constant} + \text{scale } g(t) \\ \text{scale} \end{bmatrix}$$

Table 2: SSM-Based Parameter Estimates of the Parametric Logistic Model

<i>constant</i>	<i>scale</i>	$\phi$	$\rho$	$\sigma_\epsilon^2$
3.605	1.844	1.398	0.104	0.0003

This recursion leads to the formulation of Equation 1 as an SSM with two dimensional latent state vector  $\alpha_t$ :

$$\begin{aligned}
 y_t &= [1 \ 0] \alpha_t + \epsilon_t && \text{Observation Equation} \\
 \alpha_{t+h} &= \mathbf{T}_t^{t+h} \alpha_t && \text{State Equation} \\
 \alpha_0 &= \delta && \text{Diffuse Initial Condition}
 \end{aligned} \tag{2}$$

where  $\alpha_t = [f(t); \textit{scale}]$ , the transition matrix  $\mathbf{T}_t^{t+h} = [1 \ (g(t+h) - g(t)); \ 0 \ 1]$  and, the initial condition is a two-dimensional latent vector,  $\delta$ . Note that the state equation of this SSM has no disturbance term. Standard (diffuse) Kalman filtering enables the maximum (marginal) likelihood estimation of  $\theta$  and  $\sigma_\epsilon^2$ . Once  $\theta$  and  $\sigma_\epsilon^2$  are estimated, (diffuse) Kalman smoothing enables the estimation of all latent quantities such as the initial condition  $\delta$ , and  $\alpha_t = [f(t); \textit{scale}]$  at all time points  $t$ .

As an illustration, consider the *greek\_tractors* data set considered in Garre et al. [2023]. It contains the number of tractors registered in Greece in a 45 year period between 1961 to 2006. They fit the Logistic curve to  $y = \log_{10}(\text{number of tractors})$ , by nonlinear least squares. After substituting the parameter estimates, their fitted Logistic curve has the following expression:

$$f(t) = 3.605 + 1.844 / (1 + 1.398 * \exp(-0.104 * t)) \tag{3}$$

where the time  $t$ , which starts at 0, measures years since 1961. As it turns out, fitting the same model in its state space form results in the same fit (see Table 2). Note that, in the SSM formulation only  $\phi, \rho$  and  $\sigma_\epsilon^2$  are estimated by the maximum likelihood. The other two parameters, *constant* and *scale*, are obtained as a result of Kalman smoothing. This is because, Kalman smoothing provides the estimates of the two-dimensional latent state  $\alpha_t$  at all times and *scale* is the second element of  $\alpha_t$ . Furthermore, since the first element of  $\alpha_t$  is  $f(t)$ , once *scale*,  $\phi$ , and  $\rho$  are known, *constant* can be derived from the estimate of  $f(t)$  at some convenient  $t$ , say at  $t = 0$ . Finally, Figure 1 shows the estimated Logistic fit (which matches the fit in Garre et al. [2023]) with point-wise 95% confidence band, which is also provided by the Kalman smoother.

## 2.2 SSM Formulation of a Semiparametric Growth Curve

For a variety of reasons the parametric model described in Equation 1 rarely applies perfectly in practice. Instead, a less restrictive model of the following type is often more realistic:

$$y_t = \mu_t + \epsilon_t \tag{4}$$

where the latent curve,  $\mu_t$ , is suspected to be close to a parametric, monotone curve like  $f(\theta, t)$  but not necessarily exactly equal to it. Adding a suitable disturbance term,  $\eta_t$ , in the state equation of Equation 2, provides a way to obtain such a semiparametric

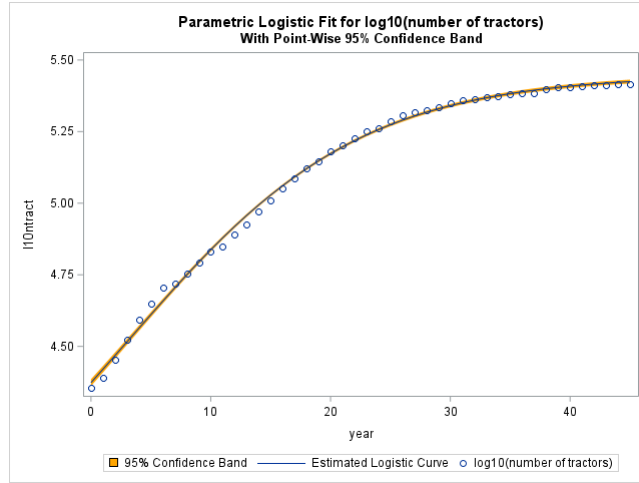


Figure 1: Parametric Logistic Fit Based on the SSM Formulation

curve:

$$\begin{aligned}
 y_t &= [1 \ 0] \boldsymbol{\alpha}_t + \epsilon_t && \text{Observation Equation} \\
 \boldsymbol{\alpha}_{t+h} &= \mathbf{T}_t^{t+h} \boldsymbol{\alpha}_t + \boldsymbol{\eta}_{t+h} && \text{State Equation} \\
 \boldsymbol{\alpha}_0 &= \boldsymbol{\delta} && \text{Diffuse Initial Condition}
 \end{aligned} \tag{5}$$

Here the state disturbances,  $\boldsymbol{\eta}_t$ , are a sequence of independent, zero-mean, two-dimensional Gaussian vectors with appropriate choice of covariance  $\mathbf{Q}_t$ . In this model the elements of the latent state vector,  $\boldsymbol{\alpha}_t$ , don't have the same interpretation as in Equation 2. Here  $\boldsymbol{\alpha}_t[1] = \mu_t$ , and  $\boldsymbol{\alpha}_t[2]$  is no longer interpretable as a simple time-invariant *scale*.

The state space formulations in Equation 2 and Equation 5 are based on the treatment of semiparametric growth-curve modeling described in Section 3 of Ansley et al. [1993]. There they describe how to obtain  $\mathbf{Q}_t$  for different choices of  $g(\boldsymbol{\theta}, t)$  so that the estimated latent curve,  $\mu_t$ , in Equation 4 satisfies a penalized least-squares criteria. However, except for some simple choices of  $g(\boldsymbol{\theta}, t)$ , obtaining a closed form expression for  $\mathbf{Q}_t$  is complicated. Instead, in this article we suggest always using the following greatly simplified form of  $\mathbf{Q}_t$ :

$$\mathbf{Q}_t^{t+h} = \sigma_\eta^2 \begin{bmatrix} \Delta^3/3 & \Delta^2/2 \\ \Delta^2/2 & \Delta \end{bmatrix} \tag{6}$$

where  $\sigma_\eta^2$  is a positive scaling factor and  $\Delta = |g(\boldsymbol{\theta}, t+h) - g(\boldsymbol{\theta}, t)|$ . We have found that this choice of  $\mathbf{Q}_t$  works well for a wide variety of  $g(\boldsymbol{\theta}, t)$  used in practice. Note that,

- The transition matrix,  $\mathbf{T}_t^{t+h}$ , used in the formulations in Equation 2 and Equation 5, is exactly the same as in Section 3 of Ansley et al. [1993].
- The choice of  $\mathbf{Q}_t$  described in Equation 6 is exact for the linear case,  $g(\boldsymbol{\theta}, t) = t$ . In the linear case, the resulting estimate of  $\mu_t$  is the well-known cubic smoothing

Table 3: SSM-Based Parameter Estimates of the Semiparametric Logistic Model

$\phi$	$\rho$	$\sigma_\eta^2$	$\sigma_\epsilon^2$
0.324	0.109	99.77	0.000

spline fit. Our recommendation of this form of  $\mathbf{Q}_t$  even for a nonlinear  $g(\boldsymbol{\theta}, t)$  is based on it being nearly optimal for a piecewise linear approximation of  $g(\boldsymbol{\theta}, t)$ .

- For the exponential case,  $g(\boldsymbol{\rho}, t) = \exp(-\rho t)$ , a closed form expression for  $\mathbf{Q}_t$  is described in Ansley et al. [1993] and an equivalent form of this model is discussed in De Jong and Mazzi [2001]. For this exponential case, we compared the growth/decay curves estimated using the exact form of  $\mathbf{Q}_t$  versus the simplified form in Equation 6 in many real and simulated data cases. In all cases the estimated curves by the exact and approximate methods matched very well. In particular, for the chlorine content data example discussed in both Ansley et al. [1993] and De Jong and Mazzi [2001], the estimated curves were essentially identical.
- When  $\sigma_\eta^2$ , the scaling factor of  $\mathbf{Q}_t$ , is either set to zero or if its estimate is nearly zero, the fully parametric case emerges. Therefore, the degree of conformity of the data to the fully parametric form can be assessed by the closeness of the estimate of  $\sigma_\eta^2$  to zero.

Continuing with the *greek\_tractors* data set, Table 3 shows the parameter estimates of the semiparametric Logistic fit. Since the estimate of the scaling factor,  $\sigma_\eta^2 = 99.77$ , is far from zero, the estimated curve,  $\mu_t$ , departs from the parametric Logistic form and the parameters  $\phi$  and  $\rho$  don't have their traditional meaning. Nevertheless, the estimate of  $\rho = 0.109$  is close to  $\rho$  in the parametric form (see Table 2). Figure 2 shows the estimated curve,  $\mu_t$ , with point-wise 95% confidence band.

In the semiparametric case, a closed form expression for  $\mu_t$ , like in Equation 3, is not possible. You can, however, evaluate  $\mu_t$  at any point  $t$  by including an (artificial) observation at that point with a missing response value. The SSM formulation handles missing response values with ease and the Kalman smoother produces appropriate estimate of  $\mu_t$  at such points.

### 2.3 FME Model With Growth Curve As a Functional Fixed-Effect

Let  $\{y_t^i, i = 1, 2, \dots, K\}$  denote longitudinal growth (or decay) measurements on  $K$  independent experimental units, which share similar environment. For example, they might denote growth patterns of puppies from the same litter, or the number of units sold over time of a new product in different (but similar) regions. The following FME model can be used to describe such data:

$$y_t^i = \mu_t + \omega_t^i + \epsilon_{i,t} \quad (7)$$

Here,  $\mu_t$ , the mean curve, is a parametric or semiparametric growth curve,  $\{\omega_t^i, i = 1, 2, \dots, K\}$  are deviation curves of the individual units from the mean curve, and  $\{\epsilon_{i,t}, i = 1, 2, \dots, K\}$  are independent,  $N(0, \sigma_\epsilon^2)$  errors. In the FME literature,  $\mu_t$  is called the functional fixed-effect and  $\omega_t^i$  are called functional-random-effects. The

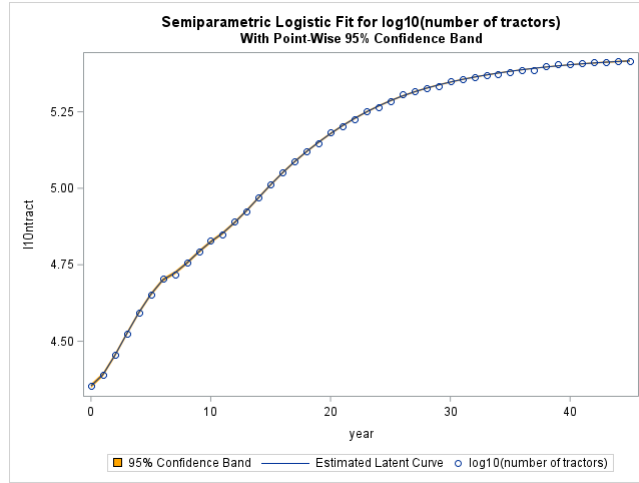


Figure 2: Semiparametric Logistic Fit Based on the SSM Formulation

deviation curves are often modeled as zero-mean, random-walks, or more elaborately as zero-mean, autoregressive processes (or something similar). For the illustrations in this article we will use zero-mean, random walks  $\{\omega_t^i\}$ , which are defined as

$$\begin{aligned}\omega_{t+h} &= \omega_t + \xi_{t+h} \\ \omega_0 &= 0\end{aligned}$$

where the disturbances  $\xi_{t+h}$  are independent  $N(0, \sigma_{dev}^2 h)$  variables ( $\sigma_{dev}^2$  is a positive scaling parameter). The FME model described in Equation 7 and much more general FME models, e.g., those with more general deviation models and with regression effects, can be easily formulated as SSMs. For now, we just describe the SSM corresponding to Equation 7 with  $\{\omega_t^i\}$  as zero-mean, random walks:

$$\begin{aligned}y_t^i &= \mathbf{Z}^i \boldsymbol{\alpha}_t + \epsilon_{i,t} && \text{Observation Equation} \\ \boldsymbol{\alpha}_{t+h} &= \mathbf{T}_t^{t+h} \boldsymbol{\alpha}_t + \boldsymbol{\eta}_{t+h} && \text{State Equation} \\ \boldsymbol{\alpha}_0 &= \begin{bmatrix} \boldsymbol{\delta} \\ 0 \end{bmatrix} && \text{Partially Diffuse Initial Condition}\end{aligned}\tag{8}$$

where the latent state vectors,  $\boldsymbol{\alpha}_t$ , are of dimension  $(2+K)$ ,  $\mathbf{Z}^i$  is a  $(2+K)$ -dimensional row vector with  $\mathbf{Z}^i[1] = 1$ ,  $\mathbf{Z}^i[2+i] = 1$  and all other elements are equal to zero,  $(2+K)$ -dimensional transition matrix  $\mathbf{T}_t^{t+h}$  is block-diagonal with the first 2-dimensional block same as that in Equation 5 and the second block is the  $K$ -dimensional identity matrix, the covariance of  $\boldsymbol{\eta}_{t+h}$ ,  $\mathbf{Q}_t^{t+h}$  is also block diagonal with the first block same as that in Equation 6 and the second block is the  $K$ -dimensional identity matrix multiplied by  $\sigma_{dev}^2 h$ .

As a quick illustration of FME model based data analysis, we analyze a small portion of the data used in Kurokawa et al. [2016]. Slightly more elaborate analysis of these data is done in Section 3. Here we consider 12 independent replicate curves generated by monitoring the growth of a bacterium strain in a nutrient rich medium

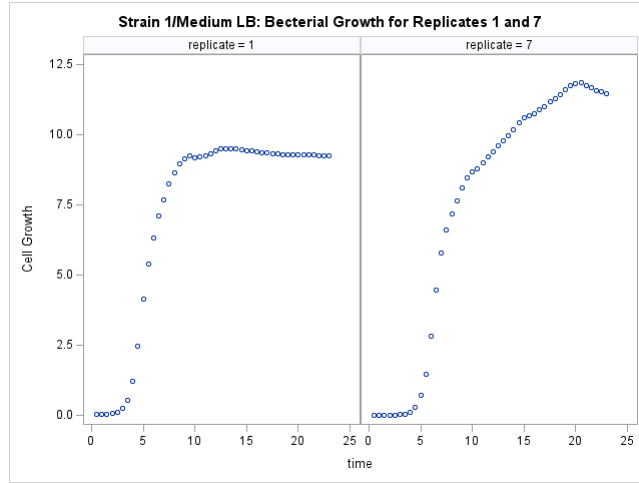


Figure 3: Bacterial growth for Strain 1 in medium LB.

Table 4: FME Model Fitting for Parametric and Semiparametric Gompertz Curves

Parametric	$Constant$	$Scale$	$\phi$	$\rho$	$\sigma_{\eta}^2$	$\sigma_{dev}^2$	$\sigma_{\epsilon}^2$	BIC
Yes	0.003	9.58	46.97	0.69	0	0.036	0.00015	-299.95
No	NA	NA	20.91	0.46	102.03	0.034	0.00014	-312.63

”NA” in a parameter column indicates that the parameter is not applicable for the model type in the corresponding row.

(strain 1, medium LB). The measurements are taken every 30 minutes during a period of 23 hours. Figure 3 shows the growth patterns for replicates 1 and 7. It shows that both the replicates loosely follow the usual sigmoidal shape, however, they do show noticeable differences in their growth patterns. We fit two FME models, one with the parametric and the other with the semiparametric Gompertz curve as a mean-curve. Table 4 shows the parameter estimates and the BIC information criteria for these two models. On the basis of BIC, the FME model based on the semiparametric Gompertz curve as a mean-curve is preferred. Figure 4 shows the mean-curve estimates based on the two models. It shows that the saturation level implied by the two models is quite different. Saturation level is often an important parameter to estimate. The estimated deviation curves highlight the difference between the replicate curves and the mean-curve. Continuing the exploration of the output from the preferred model, Figure 5 shows such deviation curves for the replicates 1 and 7. This type of examination can alert the researchers to outlying replicates.



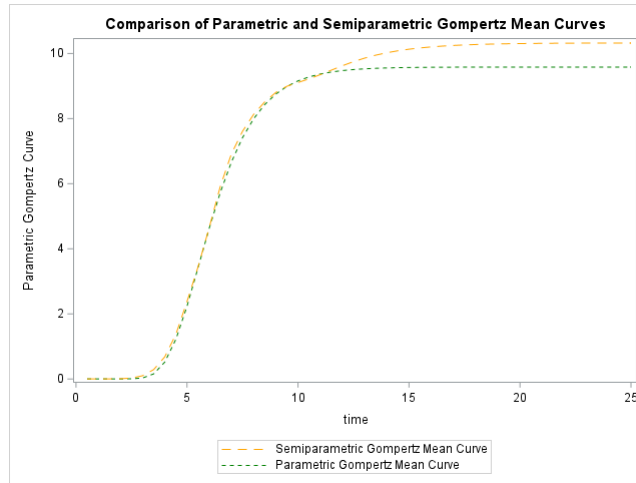


Figure 4: Comparison of mean-curve estimates of parametric and semiparametric Gompertz models

### 3 Illustration: Comparing Bacterial Growth in Different Settings

In Kurokawa et al. [2016], correlation between genome reduction and bacterial growth is studied (a link to access their data is also provided in the article). In their study, *E. Coli* cultures are grown in three settings of growth mediums and at 36 different levels of gene deletion. For each combination of growth medium and gene deletion level, multiple replicates of *E. Coli* cultures are grown. Their growth is measured at 30 minute or one hour intervals for different lengths of times. The three growth mediums are M63, MAA, and LB, which indicate poor, supplementary, and rich growth conditions, respectively. The 36 gene deletion levels are labeled as strains 1 to 36, which indicate increasing severity of gene deletion. In our illustration we will analyze the growth patterns for strains 1 and 36, grown at all the three mediums, M63, MAA, and LB (that is, total of 6 strain-medium combinations). Except in the case of (strain 36, medium M63) combination, which has 24 replicates, all other combinations have 12 replicates. Even though our methodology can easily handle different number of replicates for different combinations, we excluded the last 12 replicates for the (strain 36, medium M63) combination. Additionally, two minor adjustments to the data were made for easier viewing of the results:

- artificial observations with missing response values were added at 30 minute intervals to ensure that all the replicates have measurements on the same, uniform, time grid. This ensured that all the component estimates can be plotted in a similar way.
- all the growth measurements were multiplied by 10.0, which helped in some graphical displays.

We began our analysis by trying four FME models where the mean-curves are mod-

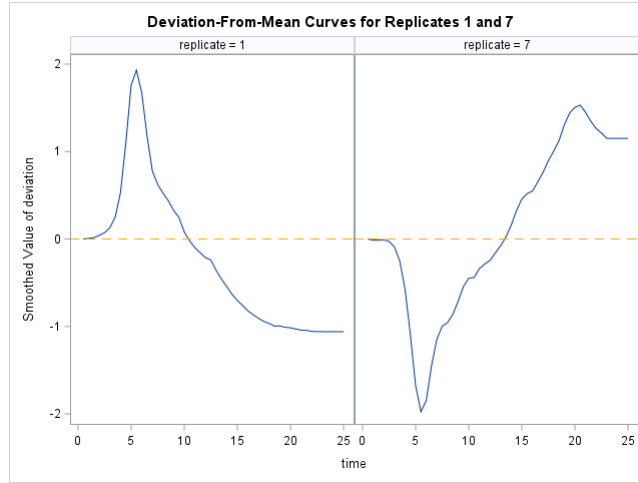


Figure 5: Deviation curves for replicates 1 and 7

Table 5: Parameter Estimates For The Chosen Models

Strain	Medium	Prior	$\phi$	$\rho$	$\nu$	$\sigma_{\eta}^2$	$\sigma_{dev}^2$	$\sigma_{\epsilon}^2$
1	M63	Logistic	9517.73	0.559	NA	244.54	0.073	0.00000
	MAA	Gompertz	39.58	0.372	NA	145.63	0.065	0.00000
	LB	Gompertz	20.91	0.463	NA	102.03	0.034	0.00014
36	M63	Gompertz	233.67	0.172	NA	366.96	0.059	0.00000
	MAA	Gompertz	7.90	0.118	NA	793.04	0.044	0.00000
	LB	Richards	71.69	0.674	0.445	0.00	0.019	0.00004

”NA” in a parameter column indicates that the parameter is not applicable for the model type in the corresponding row.

eled as semiparametric Linear, Logistic, Gompertz, and Richards curves, respectively, for each of the six strain/medium combinations. The model with best BIC criteria was chosen for each combination. Table 5 shows the chosen models and their parameter estimates. As you can see, for all the combinations a traditional growth-curve model is chosen for the mean-curve. For the (strain 36, medium LB) combination, because the estimated scaling factor  $\sigma_{\eta}^2$  is nearly zero, the mean curve turns out be a parametric Richards curve. The change in the mean curve between the least gene deletion (strain 1) and the most severe gene deletion (strain 36) for different mediums is shown in Figure 6 for M63, in Figure 7 for MAA, and in Figure 8 for LB. A few things are apparent from these plots:

- For each medium, the mean curves shift to the right and the saturation level (or the maximum level) goes down as gene deletion increases.
- In medium LB, which is the most nutrient rich, the mean curves follow the usual sigmoidal form for both strain 1 and strain 36 (see Figure 8).

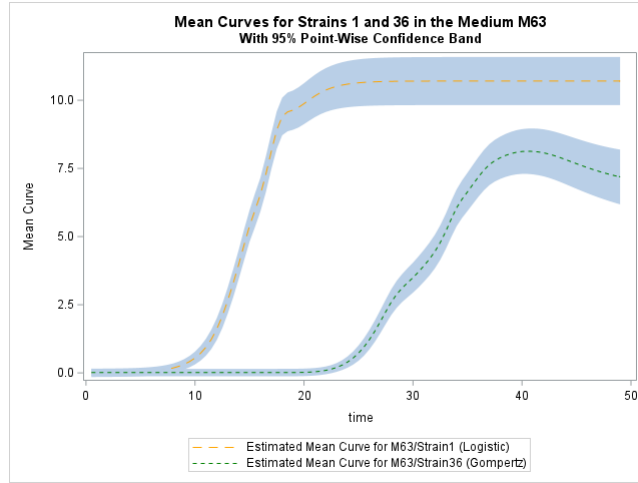


Figure 6: Change in the mean-curves from the least to most gene deletion for the medium M63

- In mediums M63 and MAA (Figure 6 and Figure 7), which are nutritionally poorer, the mean curves for Strain 1 follow the sigmoidal form. However, for Strain 36 the mean level departs significantly from the sigmoidal form and the mean level goes down after reaching its peak. That is, in these two mediums the gene deletion causes significant changes in the growth pattern.

Since all but one of these mean curves are semiparametric, the usual meanings of growth curve model parameters don't apply. So their peak growth rates, time of peak growth, etc., cannot be inferred from these parameters. Instead, these must be deduced from the estimated mean curves themselves. Since we have evaluated these mean curves, say  $\hat{\mu}_t$ , on a uniform time grid (of 30 minute interval), we can approximate their growth rate curves, say  $\hat{\lambda}_t$ , by differencing: that is,  $\hat{\lambda}_t = \hat{\mu}_t - \hat{\mu}_{t-1}$ . Table 6 shows some summary information derived from these growth rate curves. It shows that for all three mediums the peak growth rate for strain 36 is considerably lower than the peak growth rate for strain 1, moreover, in each case the peak growth rate is attained at a later time. The SSM framework can provide a lot more insight into the data. For example, it is easy to identify outlying observations and structural breaks in the components. Additionally, you can estimate difference between two component curves (e.g., the difference in the mean curves between two strain/medium combinations) and obtain confidence bands for such differences. This is useful for testing hypotheses about statistically significant differences between such curves. For this illustration also we could have continued to explore the data further but we will stop here. Of course, for the overall study, we did not analyze data for strains 2 to 35 at all. These strains could be analyzed in a similar fashion.

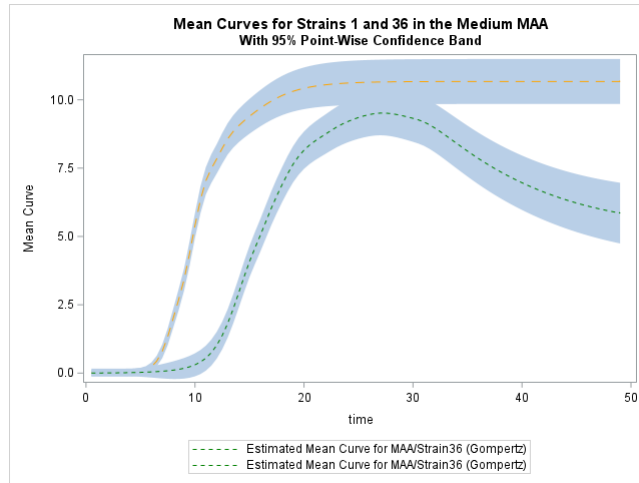


Figure 7: Change in the mean-curves from the least to most gene deletion for the medium MAA

Table 6: Maximum Growth Rates of the Mean Curves (Based on  $\hat{\lambda}_t$ )

Medium	Strain	Max Growth Rate	Attained at Time
M63	1	0.84	17.0
M63	36	0.45	33.5
MAA	1	1.03	10.0
MAA	36	0.59	14.5
LB	1	1.27	6.5
LB	36	0.88	8.0

## 4 Conclusion

We have described a flexible SSM-based framework for semiparametric modeling of growth curve data that are generated by hierarchical, longitudinal studies. Our modeling approach is based on a simplification of growth curve modeling approach that is described in Ansley et al. [1993]. We hope our treatment of their approach is more accessible and easier to adopt. The SSM-based framework described here can be easily extended in many directions. For example, the FME model in Equation 7 can contain regression effects, or additional effects that modify the mean curve to account for hormetic effects.

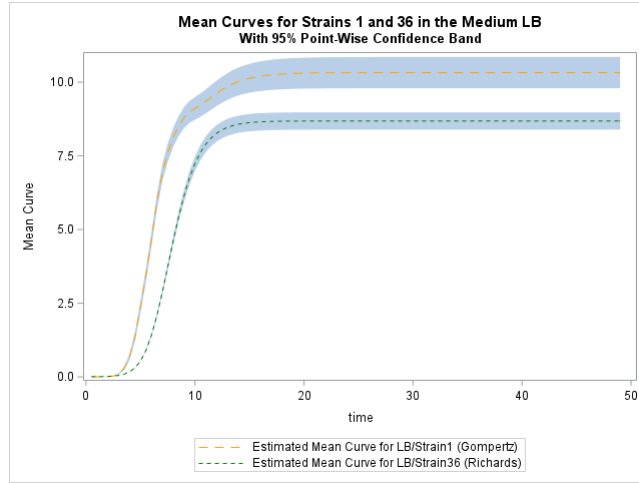


Figure 8: Change in the mean-curves from the least to most gene deletion for the medium LB

## A SSM Framework and Notation

All the SSMs discussed in this article are special cases of the following form:

$$\begin{aligned}
 \mathbf{y}_t &= \mathbf{Z}_t \boldsymbol{\alpha}_t + \mathbf{X}_t \boldsymbol{\beta} + \boldsymbol{\epsilon}_t && \text{Observation Equation} \\
 \boldsymbol{\alpha}_{t+1} &= \mathbf{T}_t^{t+1} \boldsymbol{\alpha}_t + \boldsymbol{\eta}_{t+1} && \text{State Equation} \\
 \boldsymbol{\alpha}_0 &= \boldsymbol{\eta}_0 && \text{Partially Diffuse Initial Condition}
 \end{aligned} \tag{9}$$

- $\mathbf{y}_t, t = 1, 2, \dots$  is a sequence of response vectors. The index  $t$  traverses the set  $(\tau_1 < \tau_2 < \dots)$ , which are the actual time points at which the responses are measured. The data are longitudinal and the distances between the successive time points need not be the same, that is,  $h_1 = (\tau_2 - \tau_1)$  and  $h_2 = (\tau_3 - \tau_2)$  need not be the same. The number of responses at different times, i.e., the dimension of  $\mathbf{y}_t$  at different times, need not be the same and, some or all elements of  $\mathbf{y}_t$  can be missing. In fact, missing measurements indicate that their values are to be predicted using the remaining observed data.
- The observation equation expresses the response vector as a sum of three terms:  $\mathbf{Z}_t \boldsymbol{\alpha}_t$  denotes the contribution of the state vector  $\boldsymbol{\alpha}_t$ ,  $\mathbf{X}_t \boldsymbol{\beta}$  denotes the contribution of the regression vector  $\boldsymbol{\beta}$ , and  $\boldsymbol{\epsilon}_t$  is a zero-mean, Gaussian noise vector with diagonal covariance matrix. The dimension of the state vector,  $\boldsymbol{\alpha}_t$ , does not change with time. The design matrices  $\mathbf{Z}_t$  and  $\mathbf{X}_t$  are of compatible dimensions.
- According to the state equation,  $\boldsymbol{\alpha}_{t+1}$ , the state at time  $(t + 1)$ , is a linear transformation of the previous state,  $\boldsymbol{\alpha}_t$ , plus a random disturbance,  $\boldsymbol{\eta}_{t+1}$ , which is a zero-mean, Gaussian vector with covariance  $\mathbf{Q}_t^{t+1}$  that need not be diagonal. The elements of the state transition matrix  $\mathbf{T}_t^{t+1}$  and the disturbance covariance  $\mathbf{Q}_t^{t+1}$  are known and can depend on information available at times  $t$  and  $t + 1$ .
- The initial state,  $\boldsymbol{\alpha}_0$ , is assumed to be a Gaussian vector with known mean, and covariance  $\mathbf{Q}_0$ . In many cases, no prior information about some elements of

$\alpha_0$  is available. In such cases, their variances are taken to be infinite and these elements are called diffuse.

- The noise vectors in the observation and state equations,  $\epsilon_t$ ,  $\eta_t$ , and the initial condition  $\alpha_0$ , are assumed to be mutually independent.
- The elements of system matrices  $\mathbf{Z}_t$ ,  $\text{Cov}(\epsilon_t)$ ,  $\mathbf{T}_t^{t+1}$ ,  $\mathbf{Q}_t^{t+1}$ , and  $\mathbf{Q}_0$  are assumed to be completely known, or some of them can be functions of a small set of unknown parameters (to be estimated from the data).

The latent vector  $\alpha_t$  can often be partitioned into meaningful subblocks (with corresponding blocking of the design matrix  $\mathbf{Z}_t$ ). In these cases the observation equation in Equation 9 gets the following form:

$$\mathbf{y}_t = \boldsymbol{\mu}_t + \boldsymbol{\gamma}_t + \cdots + \mathbf{X}_t \boldsymbol{\beta} + \boldsymbol{\epsilon}_t$$

where the terms  $\boldsymbol{\mu}_t$ ,  $\boldsymbol{\gamma}_t$ ,  $\cdots$  might represent a time-varying mean-level, a seasonal pattern, and so on. Such linear combinations of the state subblocks are called components. When the data from a longitudinal study is assumed to follow an SSM, the data analysis is greatly helped by the well-known (diffuse) Kalman filter and (diffuse) Kalman smoother algorithms. Chapters 4, 5, 6, and 7 of Durbin and Koopman [2012] explain how these algorithms provide the following:

- Maximum likelihood estimates of the unknown model parameters that are obtained by maximizing the marginal likelihood.
- A variety of diagnostic measures for model evaluation.
- Full-sample estimates of the latent vectors  $\alpha_t$ ,  $\boldsymbol{\beta}$ , and the model components such as  $\boldsymbol{\mu}_t, \boldsymbol{\gamma}_t, \cdots$ , at all time points. The full-sample estimates are also called the smoothed estimates in the SSM literature.
- Full-sample predictions of all missing response values.

## References

- C. F. Ansley, R. Kohn, and C. M. Wong. Nonparametric spline regression with prior information. *Biometrika*, 80(1):75–88, 1993.
- S. A. Blozis and J. R. Harring. On the estimation of nonlinear mixed-effects models and latent curve models for longitudinal data. *Structural Equation Modeling*, 23(6): 904–920, 2016.
- V. Chan, K. Tsui, Y. Wei, Z. Zhang, and X. Deng. Efficient estimation of smoothing spline with exact shape constraints. *Statistical Theory and Related Fields*, 5(1): 55–69, 2021.
- P. De Jong and S. Mazzi. Modeling and smoothing unequally spaced sequence data. *Statistical Inference for Stochastic Processes*, 4(1):53–71, 2001.
- J. Durbin and S. J. Koopman. *Time Series Analysis by State Space Methods, 2nd ed.* Oxford University Press, Oxford, 2012.
- L.F. Fine, H. Won Suk, and K. J. Grimm. An examination of a functional mixed-effects modeling approach to the analysis of longitudinal data. *Multivariate Behavioral Research*, 54(4):475–491, 2019.

- A. Garre, J. Koomen, J. den Besten, and H.M.W. Zwietering. Modeling population growth in r with the biogrowth package. *Journal of Statistical Software*, 107(1), 2023.
- W. Guo. Functional mixed effects models. *BIOMETRICS*, 58:121–128, 2002.
- A. Harvey and P. Kattuman. Time series models based on growth curves with applications to forecasting coronavirus. 1, 2020. doi: <https://doi.org/10.1162/99608f92.828f40de>.
- M. Kurokawa, S. Seno, H. Matsuda, and B. Ying. Correlation between genome reduction and bacterial growth. *DNA Research*, 23(6):425–441, 2016.
- J.O. Ramsay. Monotone regression splines in action. *Statistical Science*, 3:517–525, 1988.
- The CSSM Procedure, SAS/Econometrics User's Guide*. SAS Institute Inc., Cary, NC. [https://go.documentation.sas.com/doc/en/pgmsascdc/v\\_059/casecon/casecon\\_cssm\\_toc.htm](https://go.documentation.sas.com/doc/en/pgmsascdc/v_059/casecon/casecon_cssm_toc.htm).
- R. S. Selukar. Functional modeling of longitudinal data with the ssm procedure. In *Proceedings of the SAS Global Forum 2015 Conference*, Cary, NC, 2015. SAS Institute Inc. <https://support.sas.com/resources/papers/proceedings15/SAS1580-2015.pdf>.
- M. H. Zwietering, I. Jongenburger, F.M. Rombouts, and K. Van 'T Riet. Modeling of the bacterial growth curve. *Applied and Environmental Microbiology*, 1:1875–1881, 1990.